Resonance Raman scattering from finite and infinite polymer chains

J. Kürti
Institut für Festkörperphysik der Universität Wien, Strudlhofgasse 4, A-1090 Wien, Austria
and Department of Atomic Physics, R. Eötvös University of Budapest, H-1088 Budapest, Puskin u. 5-7, Hungary

H. Kuzmany
Institut für Festkörperphysik der Universität Wien
and Ludwig Boltzmann Institut für Festkörperphysik, Strudlhofgasse 4, A-1090 Wien, Austria
(Received 29 January 1991)

Three models for interpreting resonance Raman (RR) spectra of conjugated polymers are compared for the example of a strictly one-dimensional infinite or finite bond-alternating chain: the amplitude-mode model (AMM), the effective-conjugation-coordinate model (ECCM), and the conjugation-length model (CLM). The most characteristic behavior for the RR spectra of conjugated polymers is the change of line shape and line position of Raman modes with laser excitation energy, which is called a dispersion effect. This effect is considered to originate from inhomogeneities in the effective electron-phonon coupling constant $\tilde{\lambda}$ (AMM), in the effective force constant f_{Ja} (ECCM), or in the effective conjugation length N (CLM). Generalizing the CLM, we give a unifying picture for the three models mentioned above. The π-electron system is described by the Longuet-Higgins–Salem Hamiltonian, which includes the σ compressibility; and the RR cross section is evaluated with Albrecht's theory. By calculating $\tilde{\lambda}(N)$ and $f_{Ja}(N)$, it is shown that all inhomogeneities originate from a distribution in N. For correct calculations, no cyclic boundary conditions should be used. Extending Albrecht's theory to an infinite linear chain, we show the connection between the molecular-physics approximation (CLM) and the solid-state-physics approximation (AMM) for the RR intensity. There are two peaks in the excitation profile: one for the incoming and another for the outgoing resonance. Finally, we show that the usual Franck-Condon analysis is not appropriate for medium-long linear chains because of the dramatic difference in the shape of the total-energy hypersurface for ground and excited states.

I. INTRODUCTION

Raman spectra of conjugated polymers show some unique features. They have one or more strongly resonance enhanced bands (RR bands) which exhibit a characteristic behavior in a sense that their shape and intensity depend on the quantum energy of the exciting laser light.[1–6] If the polymer is in a state of high enough order these RR bands consist of two peaks: a primary (P) at lower and a satellite (S) at higher wave number. With decreasing laser frequency, the S peak shifts toward lower wave numbers (dispersion effect) whereas the P peak remains on the same position but gains intensity. The intensity ratio between the P and S peaks for a given laser excitation is sample dependent. Creating defects in the sample leads to a lowering of the P peak and a shift of the S peak for a given laser excitation.[7–11] A good quality *trans*-polyacetylene has, e.g., a well-separated double-peak structure if excited with a blue laser. The P-S separation is about 60 cm^{-1}. For excitation with a green laser a strong P peak with a shoulder on the high wave number side appears and for red laser excitation a very strong and single peak at the primary position is observed. Although this peculiar behavior was most intensively investigated for *trans*-polyacetylene, other conjugated polymers, such as poly(1,6-heptadiyne),[12] poly(diacetylene),[13] poly(isothianaphtene),[14] poly(methylthiophene),[15] poly(octylthiophene),[16] and poly(dihexylsilane)[17] exhibit similar properties.

The observations described above can be understood immediately if the bands for the resonance enhanced modes are assumed to originate from sample inhomogeneities. The exciting laser selects resonantly only a part of the sample and different laser lines select different parts of the polymer. The details of the inhomogeneities are model dependent. Three models have been suggested to explain the unusual resonance behavior: the conjugation-length model (CLM),[6,18,19] the amplitude-mode model (AMM),[20–22] and the effective-conjugation-coordinate model (ECCM).[23–25]

The CLM is based on a molecular quantum size picture. The conjugation length plays the central role in this model. A characteristic difference is assumed between the conjugation length and chain length[11,13] in a sense that the former is defined as the length of an unperturbed segment between defects which can be much shorter than the real chain length. The CLM considers the polymer as built up by chains with different conjugation length and this is the origin of the inhomogeneity. For example, the excitation energies depend on the segment length. For a given length the smallest excitation energy value is the HOMO-LUMO (HOMO: Highest Occupied Molecular Orbital, LUMO: Lowest Unoccupied Molecular Orbital) transition energy in the one electron MO picture. This

corresponds to the energy gap in the solid-state limit. Other parameters as transition probabilities and vibrational frequencies depend also on segment length. The RR band is the envelope of the different contributions from the various segments. The model concentrates mainly on intensities whereas the vibrational frequencies are extrapolated empirically from short oligomers.[6,26,27] The intensities are calculated using Albrecht's theory.[28,29] Electronic transition energies and matrix elements are calculated on the Hückel level,[30] Franck-Condon (FC) overlaps are calculated with the usual linear mode approximation[31] with FC parameters extrapolated from FC analysis of short oligomers.[32] With an appropriate parameter set and with a distribution function for the conjugation length the measured RR line shapes can be well fitted for laser excitation in the whole visible range.

The AMM is a solid-state approximation. The central quantity is the effective electron-phonon coupling constant $\tilde{\lambda}$ which enters the equations of motion of "bare" normal modes which are coupled to π electrons via strong electron-phonon interaction. $\tilde{\lambda}$ describes the renormalization of vibrational frequencies due to this coupling. Normal mode vibrations induce oscillations in the amplitude of the combined lattice and charge distortion (charge density wave)[33] which can be referred to as an amplitude mode (AM). The AMM considers the polymer as built up from infinite long one-dimensional chains. Inhomogeneities are introduced by assuming that various chains have various $\tilde{\lambda}$ although all are infinite long. The RR band is again the envelope of the contributions from various chains. The intensities can be calculated by usual diagrammatic technique. With a proper distribution function for $\tilde{\lambda}$ one can again reproduce the experimental RR bands.

The ECCM reformulates the AMM on the molecular physics level. The chains are quasifinite (cyclic) in this model. An effective conjugation coordinate Q_{Ja} is introduced,[23] which describes a deformation with strongest coupling with the π electrons, practically the bond alternation of the polymer backbone. The Q_{Ja} mode, the oscillation of the Q_{Ja} coordinate, in the ECCM corresponds to the AM in the AMM. This is a fictive mode which is in general not a normal mode. Any of the vibronic modes will participate to a certain amount to this mode. However, in a strictly 1D system the Q_{Ja} mode can be assigned to an eigenmode of the system. $\tilde{\lambda}$ of AMM can be expressed by a microscopic force constant in the ECCM. The dominant role in the force constant matrix is played by the force constant f_{Ja} of the effective conjugation coordinate. f_{Ja} is the renormalized bond stretching force constant which is different for different chain lengths. The calculations are based on a reduced version of the well-known *GF* method.[34] The ECCM concentrates mainly on the positions and on the relative intensities of various RR bands.

The aim of this paper is to compare the three models, find connections between them, and analyze advantages and disadvantages for special applications. Another goal was to study the approach of the molecular description to the solid-state limit in detail. In order to do this Albrecht's theory was extended to quasi-infinite chains. Because the resonance Raman phenomenon is complicated by itself, a very simply system consisting of an idealized strictly linear bond alternating chain was chosen in order to obtain quantitative results. For an infinite number of bonds this is the well-known Peierls chain.[35,36] The π electrons were described by the Longuet-Higgins–Salem (LHS) model which takes the σ compressibility into account and thus allows geometry optimization.[37–40] The LHS model allows one to compute all electronic and vibronic parameters which are needed to describe the resonance Raman effect. The RR intensity was calculated by a general second-order perturbation treatment according to Albrecht's approximations.[28,29] Some preliminary results were published recently.[41]

In this paper we first summarize the main points of Albrecht's theory. In Sec. III we apply it to the finite LHS chain and then extend it to the infinite Peierls chain. In Sec. IV A we review the AMM, compare it with Albrecht's results for infinite chains, and discuss the possibility to use it for finite chains. This, together with the results of Sec. III, can be regarded as a generalization of the CLM. In Secs. IV B and IV C we summarize the concept for the ECCM and for the original CLM and compare them with results of Sec. III. Section V discusses the question which model is closest to real polymer systems and summarizes the results.

From the analysis we found that the intensities computed by Albrecht's theory in the limit of infinite chains reproduce the intensities computed by AMM if in the latter the phonon frequency is not neglected as compared to the characteristic electronic energies (energy gap). The use of the AMM for finite chains is conceptionally problematic because the model is intimately connected with translational symmetry which does not exist in finite systems. For the same reason the ECCM is correct only qualitatively since it only simulates finite chains by restricting the interaction between unit cells to a finite distance but using translational symmetry. However, we show that it is possible to define the Q_{Ja} mode for real finite chains without periodic boundary conditions. The CLM is conceptionally the most realistic among the three models. It uses explicit calculations for the FC approximation to evaluate the Raman intensities. However, we show that at least for the simple case of a strictly one-dimensional chain investigated in this paper, a conventional FC approximation cannot be performed for medium long chains because the total energy hypersurface for the excited states differs very much from that of the ground state. The reason for this behavior is most probably the strong tendency of the geometry in the excited state to relax into a completely different geometry containing a soliton-antisoliton pair.

II. GENERAL PERTURBATION TREATMENT OF THE RESONANCE RAMAN PROCESS

Because we want to investigate whether the molecular physics description of the resonance Raman process in the infinite limit converges to the solid-state description we briefly summarize the main assumptions and results of Albrecht's theory for Raman processes in molecules.

Figure 1 shows a generalized Raman process, which is an inelastic scattering of light on an arbitrary microscopic system.[42] The latter is in the energy eigenstate $|\mathcal{I}\rangle$ and $|\mathcal{F}\rangle$ before and after interaction with light, respectively. There is one photon with energy $\omega_{\mathcal{I}}$ ($\hbar=1$ is used) before and another one with energy $\omega_{\mathcal{F}}$ after the interaction. The interaction Hamiltonian between a charged particle and electromagnetic field is in the nonrelativistic limit the sum of $\hat{K}_{\mathrm{I}}$ and $\hat{K}_{\mathrm{II}}$ where

$$\hat{K}_{\mathrm{I}}=\frac{e}{mc}\hat{\mathbf{p}}\cdot\hat{\mathbf{A}} \quad \text{and} \quad \hat{K}_{\mathrm{II}}=\frac{e^2}{2mc^2}\hat{\mathbf{A}}^2 . \tag{1}$$

The vector potential $\hat{\mathbf{A}}$ of the radiation can be expanded into plane waves:

$$\hat{\mathbf{A}}\propto\sum_{\mathbf{q},s}\boldsymbol{\epsilon}_{\mathbf{q},s}(\hat{a}_{\mathbf{q},s}e^{i\mathbf{q}\cdot\mathbf{r}}+\hat{a}^{\dagger}_{\mathbf{q},s}e^{-i\mathbf{q}\cdot\mathbf{r}} . \tag{2}$$

$\hat{a}_{\mathbf{q},s}$ and $\hat{a}^{\dagger}_{\mathbf{q},s}$ are the annihilation and creation operators, respectively, for a photon with wave vector $\mathbf{q}$ and polarization vector $\boldsymbol{\epsilon}_{\mathbf{q},s}$. It can be shown that in Coulomb gauge and for interaction of visible light with electrons bounded in molecules $\hat{K}_{\mathrm{II}}$ is much weaker than $\hat{K}_{\mathrm{I}}$ and can be neglected.[43] Then, the probability of the process illustrated on Fig. 1 is the square of the amplitude with $\hat{K}_{\mathrm{I}}$ which can be expressed as a perturbation series with the leading terms

$$\sum_{\mathcal{V}}\frac{\langle\omega_{\mathcal{F}};\mathcal{F}|\hat{K}_{\mathrm{I}}|0;\mathcal{V}\rangle\langle 0;\mathcal{V}|\hat{K}_{\mathrm{I}}|\omega_{\mathrm{I}};\mathcal{I}\rangle}{E_{\mathcal{V}}-(E_{\mathcal{I}}+\omega_{\mathcal{I}})} \tag{3a}$$

and

$$\sum_{\mathcal{V}}\frac{\langle\omega_{\mathcal{F}};\mathcal{F}|\hat{K}_{\mathrm{I}}|\omega_{\mathcal{F}}\omega_{\mathcal{I}};\mathcal{V}\rangle\langle\omega_{\mathcal{F}}\omega_{\mathcal{I}};\mathcal{V}|\hat{K}_{\mathrm{I}}|\omega_{\mathcal{I}};\mathcal{I}\rangle}{(E_{\mathcal{V}}+\omega_{\mathcal{I}}+\omega_{\mathcal{F}})-(E_{\mathcal{I}}+\omega_{\mathcal{I}})} \tag{3b}$$

with the corresponding diagrams Figs. 2(a) and 2(b), respectively. With $E_{\mathcal{I}}+\omega_{\mathcal{I}}\equiv E_{\mathcal{F}}+\omega_{\mathcal{F}}$ the sums in Eqs. (3a) and (3b) consist of individual terms of the form $1/[(E_{\mathcal{V}}-E_{\mathcal{I}})-\omega_{\mathcal{I}}]$ and $1/[(E_{\mathcal{V}}-E_{\mathcal{F}})+\omega_{\mathcal{I}}]$. In Eqs. (3a) and (3b) $|\mathcal{V}\rangle$ denotes an arbitrary excited state of the microscopic many-electron–many-nuclei system. The expressions contain matrix elements of the type

$$\langle 0,\mathcal{V}|\hat{K}_{\mathrm{I}}|\omega_{\mathcal{I}},\mathcal{I}\rangle\propto\frac{1}{\sqrt{\omega_{\mathcal{I}}}}\left\langle\mathcal{V}\left|\sum_k\frac{e_k}{m_k}\boldsymbol{\epsilon}_{\mathbf{q},s}\mathbf{p}^{(k)}e^{i\mathbf{q}\cdot\mathbf{r}^{(k)}}\right|\mathcal{I}\right\rangle , \tag{4}$$

where the sum runs over the particles with charge e_k in the molecule. In the dipole approximation the exponential term is 1 for molecules with a size much smaller than the wavelength of the incident light.[44] In the case of a strictly linear chain it is even exactly correct since light polarization must be parallel to the chain and thus light propagation is perpendicular to the chain. Using the well-known identity

$$\left\langle\mathcal{V}\left|\frac{e}{m}\hat{\mathbf{p}}\right|\mathcal{I}\right\rangle=i(E_{\mathcal{V}}-E_{\mathcal{I}})\langle\mathcal{V}|e\hat{\mathbf{r}}|\mathcal{I}\rangle \tag{5}$$

and after some algebra[29] one obtains the well-known expression for the intensity I of scattered light with polarization ρ, if the incoming light has intensity I_0 and polarization σ

$$I_{\rho}\propto I_{0\sigma}\omega_{\mathcal{F}}^4|\alpha_{\rho\sigma}|^2 , \tag{6}$$

where $\alpha_{\rho\sigma}$ is the transition polarizability of the molecule

$$\alpha_{\rho\sigma}=\sum_{\mathcal{V}}\left[\frac{\langle\mathcal{F}|\hat{M}_{\rho}|\mathcal{V}\rangle\langle\mathcal{V}|\hat{M}_{\sigma}|\mathcal{I}\rangle}{(E_{\mathcal{V}}-E_{\mathcal{I}})-\omega_{\mathcal{I}}+i\Gamma_{\mathcal{V}}}+\frac{\langle\mathcal{F}|\hat{M}_{\sigma}|\mathcal{V}\rangle\langle\mathcal{V}|\hat{M}_{\rho}|\mathcal{I}\rangle}{(E_{\mathcal{V}}-E_{\mathcal{F}})+\omega_{\mathcal{I}}+i\Gamma_{\mathcal{V}}}\right] . \tag{7}$$

For strictly linear chains only α_{zz} is nonzero where z is the chain direction. In Eq. (7) $\hat{M}$ is the sum of the electronic and nuclear dipole moments

$$\hat{\mathbf{M}}=\hat{\mathbf{M}}_{\mathrm{el}}+\hat{\mathbf{M}}_{\mathrm{nucl}}=e\sum_k\hat{\mathbf{r}}^{(k)}-e\sum_l Z_l\hat{\mathbf{R}}^{(l)} . \tag{8}$$

Equation (7) is a general result from the perturbation theory. $|\mathcal{I}\rangle$, $|\mathcal{V}\rangle$, and $|\mathcal{F}\rangle$ are energy eigenstates of the whole molecule including electrons and nuclei. Albrecht's theory is the evaluation of Eq. (7) for a system for which the Born-Oppenheimer approximation is valid. In this case the total molecular wave function is a product of a many-electron wave function and that of a nuclear wave function. The nuclear motion is treated as usual in the harmonic approximation. In the Raman process the *electronic* wave function is identical in the initial and in the final state: $|g\rangle$. In the nuclear final state there is one vibronic quantum more (Stokes) or less (anti-

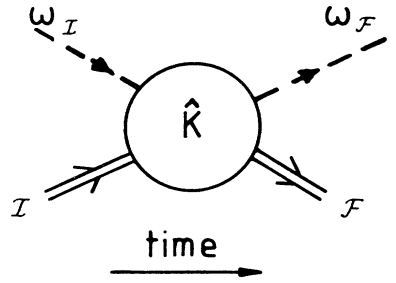

FIG. 1. Generalized Raman process for a system in initial state $\mathcal{I}$ and final state $\mathcal{F}$ and incident and scattered radiation $\omega_{\mathcal{I}}$ and $\omega_{\mathcal{F}}$, respectively.

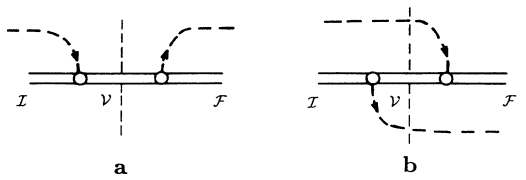

FIG. 2. Lowest order diagrams for a generalized Raman process described by $\hat{K}_{\mathrm{I}}$ for the two possible time orders [according to Eqs. (3a) and (3b)].

Stokes) than in the initial state. The corresponding states can be written as

$$|\mathcal{I}\rangle = |g;i\rangle = |g\rangle\,|\{i\}^g\rangle\ , \tag{9a}$$

$$|\mathcal{V}\rangle = |e;v\rangle = |e\rangle\,|\{v\}^e\rangle\ , \tag{9b}$$

$$|\mathcal{F}\rangle = |g;f\rangle = |g\rangle\,|\{f\}^g\rangle\ . \tag{9c}$$

The nuclear dipole momentum operator has nonzero matrix elements only if there is no change in the many-electron state therefore it does not play any role in RR processes where ($e \neq g$). The electronic dipole momentum operator acts only on the electronic wave functions but due to their dependence on nuclear coordinates (normal modes) the electronic dipole matrix element still acts as operator for the vibronic normal modes:

$$\langle e;v|\hat{\mathbf{M}}_{\rm el}|g;i\rangle = \langle\{v\}^e|\mathbf{M}_{e,g}(\{Q\})|\{i\}^g\rangle\ . \tag{10}$$

In the Franck-Condon approximation the dipole matrix element is considered to be constant and replaced with its value in the ground-state equilibrium nuclear configuration:

$$\mathbf{M}_{e,g}(\{Q\}) \approx \mathbf{M}^0_{e,g,}\ . \tag{11}$$

The remaining overlaps are the so called FC integrals:

$$\langle\{v\}^e|\{i\}^g\rangle\ . \tag{12}$$

Usually the multidimensional FC integral is factorized with respect to the ground-state normal modes. Assuming that the only difference between potential energy curves in the ground state and in the excited state is that their minimum positions are shifted (see Fig. 3) the FC integrals can be expressed as[31]

$$\langle\Phi^e_\beta|\Phi^g_\alpha\rangle = e^{-z^2/2}\left[\frac{\alpha!}{\beta!}\right]^{1/2} z^{\beta-\alpha}L^{\beta-\alpha}_\alpha(z^2)\ , \tag{13}$$

where L^k_i are Laguerre polynoms and $z \equiv a/\sqrt{2}$ is the dimensionless FC parameter. a is the shift between the two

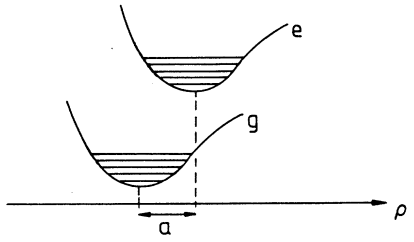

FIG. 3. Total energy curves for electronic ground state (g) and excited state (e) as a function of a dimensionless ground-state normal coordinate ρ. In the simplest case there is only a shift a between two minima.

quadratic curves in Fig. 3 measured in dimensionless normal coordinate $\rho = \sqrt{m\Omega}\cdot Q$.

Optical experiments are often analyzed successfully based on the FC assumption. For a general description of the Raman processes, however, the assumption of constant dipole matrix element [Eq. (11)] is not good enough. Thus the next approximation is the Herzberg-Teller expansion[45] of the matrix element into linear terms in the normal coordinates:

$$\mathbf{M}_{e,g}(\{Q\}) \approx \mathbf{M}^0_{e,g} + \sum_a \mathbf{M}^1_{e,g;a}Q_a\ . \tag{14}$$

For the case of the linear chain the matrix elements

$$M^1_{e,g;a} = \left.\frac{\partial M_{e,g}}{\partial Q_a}\right|_0 \tag{15}$$

can be directly computed. Substituting Eqs. (10) and (14) into Eq. (7) one can get the A, B, and C terms of Albrecht's theory:

$$(\alpha_{\rho\sigma})_{gi,gf} = A + B + C = (A_- + A_+) + B + C\ , \tag{16}$$

where

$$A_- = \sum_{e,v}\left[\frac{1}{E_{e,v} - E_{g,i} - \omega_L + i\Gamma_{e,v}}\right](M_\rho)^0_{e,g}(M_\sigma)^0_{e,g}\langle\{f\}^g|\{v\}^e\rangle\langle\{v\}^e|\{i\}^g\rangle\ , \tag{17a}$$

$$A_+ = \sum_{e,v}\left[\frac{1}{E_{e,v} - E_{g,f} + \omega_L + i\Gamma_{e,v}}\right](M_\rho)^0_{e,g}(M_\sigma)^0_{e,g}\langle\{f\}^g|\{v\}^e\rangle\langle\{v\}^e|\{i\}^g\rangle\ , \tag{17b}$$

$$B = (B_-) = \sum_{e,v}\left[\frac{1}{E_{e,v} - E_{g,i} - \omega_L + i\Gamma_{e,v}}\right]\Sigma(a)\ , \tag{17c}$$

$$C = (B_+) = \sum_{e,v}\left[\frac{1}{E_{e,v} - E_{g,f} + \omega_L + i\Gamma_{e,v}}\right]\Sigma(a)\ , \tag{17d}$$

and

$$\Sigma(a) = \sum_a\left[(M_\rho)^0_{e,g}(M_\sigma)^1_{e,g;a}\langle\{f\}^g|\{v\}^e\rangle\langle\{v\}^e|Q_a|\{i\}^g\rangle + (M_\rho)^1_{e,g;a}(M_\sigma)^0_{e,g}\langle\{f\}^g|Q_a|\{v\}^e\rangle\langle\{v\}^e|\{i\}^g\rangle\right]\ .$$

These formulas hold for general Raman processes. In the resonance case one or a few terms in A_- and B_- dominate for which the denominator is almost zero because the quantum energy of the light is nearly equal to a real electronic excitation energy. Thus, for a resonance Raman process C and A_+ terms can be neglected. Furthermore, for the investigation of small molecules under resonance conditions the B term is usually also neglected. On the contrary, as it will be shown in Sec. III C, for infinite linear chains only the B term differs from zero and thus describes the solid state approach.

III. RESONANCE RAMAN PROCESS FOR LINEAR CHAINS (GENERALIZED CLM)

To evaluate the terms in Eqs. (17) it is necessary to calculate the electronic and vibronic eigenstates and eigenvalues. In order to be able to compute all parameters needed a simple system, a linear chain described by the LHS model[37–40] was considered. On the other hand, this paragraph can be regarded as the generalization of the conventional conjugation length model because not only the electronic properties are calculated but a normal coordinate analysis is done as well.

A. Evaluation of energies, matrix elements, and normal coordinates in the LHS approximation

We consider a CH chain simplified to a strictly one-dimensional geometry according to Fig. 4. An oligomer with N carbon atoms is replaced by a linear chain of N atoms with masses of $m_{CH_2}=25729$ a.u. (the free-electron mass is 1 a.u.) at the ends of the chain and $m_{CH}=23892$ a.u. for the others. The geometry is allowed to change only within the $(N-1)$-dimensional configuration space spanned by the bond lengths $r_1, r_2, \ldots, r_{N-1}$. We consider the interaction of the light only with the N π electrons. The σ electrons contribute to the total energy by an additive term which depends on the actual geometry. The π electrons are treated on a tight-binding Hückel level. The following approximations have been used:

Born-Oppenheimer approximation.

σ-π separation.

One-electron approximation.

Linear combination of atomic orbitals (LCAO's) for the molecular orbitals with one orbital per site.

Zero overlap between different atomic orbitals.

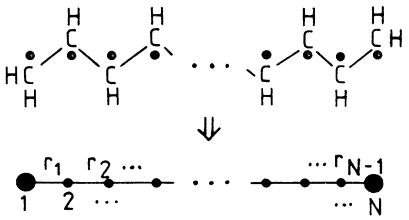

FIG. 4. Simplifying an oligomer with N carbon atoms to a strictly one-dimensional finite chain. The individual bond lengths $r_1, r_2 \cdots r_{N-1}$ can have different values. The masses of the atomic cores at the chain ends are m_{CH_2}, all others are m_{CH}.

In the Hückel approximation the π-electron Hamiltonian is an $N \times N$ matrix in the space of the linear combination factors of the atomic orbitals. The total π-electron energy is in the above approximation the sum of the one-electron energies ε_i weighted by the occupation number of the corresponding molecular orbital ($n_i=0,1$ or 2):

$$E_{\pi,\mathrm{tot}}=\sum_i \varepsilon_i \cdot n_i = \sum_i \left[\sum_j \beta_j (C_j^{(i)*} C_{j+1}^{(i)} + C_{j+1}^{(i)*} C_j^{(i)})\right] n_i \ , \tag{18}$$

where $C_j^{(i)}$ are the LCAO coefficients and β_j is the resonance integral for the jth bond. The quantity which characterizes the strength of a π bond is the mobile bond order p_j with the definition

$$p_j=\tfrac{1}{2}\sum_i (C_j^{(i)*} C_{j+1}^{(i)} + C_{j+1}^{(i)*} C_j^{(i)}) n_i \ . \tag{19}$$

p_j is 0 and 1 for a pure single bond (ethene) and double bond (ethylene), respectively, and falls in between these values on the general case. Substituting Eq. (19) into Eq. (18) yields

$$E_{\pi,\mathrm{tot}}=2\sum_j \beta_j p_j \ , \tag{20}$$

where the sum runs over all bonds. On the other hand for fixed occupation numbers $E_{\pi,\mathrm{tot}}$ is a first-order homogeneous function of the β_j, from which together with Eq. (20) immediately follows:

$$p_j=\frac{1}{2}\frac{\partial E_{\pi,\mathrm{tot}}}{\partial \beta_j} \ . \tag{21}$$

So far the results are well known in the usual Hückel theory. Longuet-Higgins and Salem generalized the Hückel theory by including the σ electrons (σ compressibility) and by allowing a change in the resonance integral with changing bond length assuming a well-defined monotonic correspondence between them. Thus in the LHS model

$$E_{\mathrm{tot}}=E_{\pi,\mathrm{tot}}(\{r\})+E_{\sigma,\mathrm{tot}}(\{r\}) \ , \tag{22a}$$

where

$$E_{\pi,\mathrm{tot}}=2\sum_j \beta_j(r_j) p_j(\{r\},\{n\}) = E_{\pi,\mathrm{tot}}(\beta_1(r_1);\ldots;\{n\}) \ , \tag{22b}$$

$$E_{\sigma,\mathrm{tot}}=\sum_j f_j(r_j) \ . \tag{22c}$$

In Eq. (22b) $\{n\}$ is the set of the occupation numbers. In Eq. (22c) $f(r)$ is the potential energy of the σ core. $\beta(r)$ can be reasonably assumed as an exponential function:

$$\beta(r)=-A_\beta \exp\left[-\frac{r}{B_\beta}\right] \ . \tag{23}$$

$f(r)$ can be obtained from ground-state equilibrium considerations. The first derivatives of the total energy are zero at the equilibrium geometry:

$$\frac{\partial E_{\text{tot}}}{\partial r_i}=\frac{df_i}{dr_i}+\frac{\partial E_{\pi,\text{tot}}}{\partial \beta_i}\cdot\frac{d\beta_i}{dr_i}=0 \ . \tag{24}$$

Using Eqs. (23) and (21), from Eq. (24) immediately follows that there is a one to one correspondence between bond length r and bond order p. Assuming the empirically observed linear bond length-bond order relation[46] (Coulson relation)

$$r=R_1-(R_1-R_2)p \tag{25}$$

as exact, the $f(r)$ function can be obtained from Eqs. (24), (23), and (25):

$$f(r)=\frac{2}{R_1-R_2}\beta(r)(r-R_1+B_\beta) \ . \tag{26}$$

R_1 and R_2 are the lengths of a pure single and double bond, respectively. Even though $f(r)$ is obtained from a ground-state configuration one can use this function for all π excitations as well because of the assumed σ-π separation. The LHS model is characterized by Eqs. (22), (23), and (25) or 26. The bond lengths can be optimized self-consistently by satisfying the Coulson relation which at the same time minimizes the total energy. With the LHS model it is straightforward to describe, e.g., the appearance of bond alternation in linear chains or topological defects such as solitons or polarons.[38,47]

There are only four parameters in the model: R_1, R_2, A_β, and B_β which were determined as follows. The single and double bond lengths were taken from the literature: $R_1=1.54$ Å, $R_2=1.33$ Å. The bond length alternation for very long chains scales with B_β, independent from A_β. A choice of $B_\beta=0.3075$ Å leads to a bond alternation for the infinite chain of 1.36 Å/1.45 Å which is in reasonable agreement with the experimentally observed values in *trans*-polyacetylene.[48] For fixed B_β the energy gap (HOMO-LUMO difference) scales with A_β. A choice of $A_\beta=243.5$ eV leads to the value of 1.5 eV which is again in reasonable agreement with the experimentally observed gap in *trans*-polyacetylene.[49] It should be mentioned that the LHS model can after some generalization successfully describe more complicated systems with heteroatoms like, e.g., poly(isothianaphthene).[40,50]

To calculate the Raman intensities the electronic dipole matrix elements are also required. The many-electron matrix element for Slater determinant wave functions is nonzero only if one electron is excited. The one-electron dipole matrix element between ith and jth molecular orbital can be easily evaluated using the assumption of the orthogonality of atomic orbitals:

$$\langle j|\hat{\mathbf{M}}|i\rangle=e\sum_m C_m^{(j)*}C_m^{(i)}\mathbf{r}^{(m)} \ , \tag{27}$$

where $\mathbf{r}^{(m)}$ is the position of the mth nucleus. In addition, Eqs. (17) require the FC integrals which needs a vibronic normal coordinate analysis. The LHS model is capable for this purpose too. For Wilson's well-known *GF* formalism[34] the $\hat{F}$ force constant matrix

$$F_{ij}=\frac{\partial^2 E_{\text{tot}}}{\partial r_i \partial r_j} \tag{28}$$

and the $\hat{G}$ reciprocal mass matrix

$$G_{ij}=\sum_k \frac{1}{m_k}B_{ik}B_{jk} \tag{29}$$

are needed. Both are $(N-1)\times(N-1)$ matrices for an N-atomic linear chain. In Eq. (29) the $\hat{B}$ matrix makes the connection between internal coordinates (bond length changes dr_i) and Cartesian coordinates (atomic position changes dx_i) $dr_i=\sum_j B_{ij}\cdot dx_j$ $(i=1,\ldots N-1;\ j=1,\ldots N)$. The vibronic normal modes and normal frequencies are the eigenvectors and eigenvalues of the following equation:

$$\hat{G}(N)\hat{F}(N)\cdot\mathbf{Q}(N)=\Omega^2(N)\cdot\mathbf{Q}(N) \ . \tag{30}$$

For the infinite long chains the only Raman modes are those which are totally symmetric and have wave vector $k=0$.[51] In our case the infinite linear chain is uniformly dimerized and the only Raman active mode is the one where all atoms vibrate with the same amplitude "u" and the neighboring atoms vibrate in the opposite phase as seen in Fig. 5. Thus, this mode is the amplitude mode in the AMM and the *Ja* mode in the ECCM as it was mentioned in the Introduction and will be discussed in Secs. IV A and IV B. For the finite chain the situation is much more complicated but for symmetry reasons there is always one and only one normal mode where the neighboring atoms vibrate in the opposite phase although the magnitude of the vibration is not uniform along the chain. We define this mode as the *Ja mode of the finite chain* since for the limit $N\to\infty$ it converges to the *Ja* mode of Fig. 5. Thus, from an evaluation of the eigenvectors of Eq. (30) it is straightforward to select the Q_{Ja} mode for the finite chain. Because this is the only mode which is important in the resonance Raman behavior of very long chains, we concentrated on this mode for short chains as well. The change of ith bond length during the vibration according to the *Ja* mode can be expressed as $dr_i=q_{Ja}\cdot(Q_{Ja})_i$, where $\sum_i|(Q_{Ja})_i|^2=1$. We were interested in the change of the properties of the *Ja* mode as a function of N. As an example Table I shows the components of the normal modes for a chain of four atoms as obtained from Eq. (30). In this case Q_3 is Q_{Ja}. Characteristic for Q_{Ja} of long chains is that its components are almost zero at the ends and tend to be constant in absolute value at the center of the chain as it would be expect-

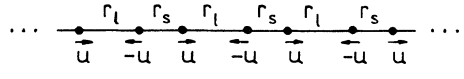

FIG. 5. Q_{Ja} mode of an infinite chain or a finite chain with cyclic boundary conditions. r_l and r_s are the long and short bonds in the unit cell, u is the uniform vibrational amplitude.

TABLE I. Normalized bond length changes of the three vibrational normal modes of a chain with four atoms.

Bond	Q_1	Q_2	$Q_3 \equiv Q_{Ja}$
1	0.2876	−0.7071	−0.5254
2	0.9135	0	0.6693
3	0.2876	0.7071	−0.5254

ed for the infinite case. Table II shows this tendency for a chain of 100 atoms. In the next paragraphs the Raman properties of the Q_{Ja} mode of linear chains will be investigated for finite and infinite chains.

B. Albrecht's theory for finite linear chains

With the model developed above one can calculate the resonance Raman characteristics of a linear chain as a function of the chain length. As far as the Raman line position is concerned it is straightforward. The details of the frequency analysis will be discussed in Secs. IV A and IV B where we compare our results with those of the AMM and ECCM. The Raman intensity can be also calculated in principle, using Eqs. (17). However, serious problems arise in calculating vibronic overlaps as it is shown in this paragraph.

Considering only the Q_{Ja} normal mode it is possible to calculate all quantities in Eqs. (17) which are necessary to evaluate Albrecht's A and B terms. Table III collects these values at least for the first two electronic excitations ($k=1$: HOMO to LUMO, $k=2$: HOMO-1 to LUMO$+1$) for different chain lengths from $N=4$ to 120. Only the "symmetrical" one electron excitations—where the initial state is by the same amount below the Fermi level as the final state above it—have nonzero matrix elements. The decrease and final saturation for the transition energies and the increase and final saturation for the transition matrix elements with increasing N are characteristic for Hückel theory. The first derivative of the matrix elements are smaller than the matrix elements themselves so that the usual neglection of Albrecht's B term is a good approximation.

A surprising result from Table III is the behavior of the FC parameter z together with the ratio of the curvature of the total energy curves in the excited and in the ground state if the chain is longer than 10, at least for the HOMO-LUMO excitation. These results can be more clearly seen in Fig. 6 which shows the corresponding total energy curves for $N=4$, 10, 50, and 120 as a function of the dimensionless Ja coordinate $\rho_{Ja}=\sqrt{m_{Ja}\Omega_{Ja}}\cdot q_{Ja}$, where Ω_{Ja} and q_{Ja} are the frequency and amplitude of the Ja mode, respectively, and m_{Ja} is calculated according to Eq. (47b). The figure illustrates that beginning with about $N=10$ the total energy curve in the excited state starts to deviate from quadratic in ρ_{Ja} and becomes more and more anharmonic with increasing N. This means that for increasing N the usual FC analysis [see Eqs. (12) and (13)] cannot be carried out satisfactorily any more. The analysis finally becomes impossible for $N \geq 40$. As will be shown later, for $N \gg 100$ the potential energy becomes harmonic again.

To understand the reason for this behavior the following must be considered. In the first excited state the bond lengths in the configuration for which the total energy has a minimum differs very much from the ground-state minimum energy geometry. On a long chain the minimum energy configuration for the first excited state corresponds to a soliton-antisoliton pair at optimum distances from each other and from the chain ends. The distance over which the inverted bond alternation is extended is about 14 atoms. The tendency to relax in the first excited state into a completely different geometry as compared to the ground-state geometry means that the total energy hypersurface in the excited state can differ very much from that for the ground state. As a consequence the ground-state normal modes are no longer proper normal modes for the excited state, a strong "Dushinsky rotation"[52] takes place. The total energy curve can differ very much from a parabola if the first excited state energy hypersurface is cut along the direction which is the ground state Q_{Ja} normal mode (see Fig. 6, $N=50$). In this case the multidimensional FC integrals cannot be factorized into one-dimensional overlaps with respect to the ground-state normal modes. For very short chains the effect is not so strong because the "solitonlike" geometry is hardly established. There is not enough space to form a "real" soliton-antisoliton pair and thus, it does not perturb essentially the potential energy in the excited state. On the other hand, as it will be shown in Sec. III C, for the *infinite* chain the effect of the soliton geometry, which is a localized distortion, is negligible on the FC analysis with respect to the Q_{Ja} normal mode, which is a delocalized effect along the whole chain. This holds even though the deepest minimum may be at a different position in ground and excited states in this case as well. Numerical analysis shows indeed that for chains longer than $N=100$ again a small minimum in the excited state potential appears which becomes deeper for longer chains. Figure 6 shows this for $N=120$

C. Extension of Albrecht's theory to infinite linear chain

We now investigate an infinite chain with uniform bond length alternation where the only allowed change in the geometry is the Q_{Ja} mode as it was illustrated on Fig. 5. The infinite chain can be considered as the limiting case of finite chains but with cyclic boundary conditions. With respect to uniformity of bond alternation and Q_{Ja} along the ring the same holds as for the infinite chain. However, the cyclic boundary conditions permit the con-

TABLE II. The components of Q_{Ja} normal mode for a chain with 100 atoms.

Bond (i)	1	2	3	···	49	50	51	···
$(Q_{Ja})_i$	−0.002	0.003	−0.005	···	−0.148	0.148	−0.148	···

TABLE III. Parameters used in Albrecht's A and B terms corresponding to the first two electronic transitions ($k=1$: HOMO $\rightarrow$ LUMO, $k=2$: HOMO $-1\rightarrow$ HOMO$+1$) for several chain lengths (N). $\sqrt{2}\cdot z$ is the shift between minima of the potential curves measured in the dimensionless amplitude of the Q_{Ja} normal mode, $\sqrt{f_e/f_g}$ is the ratio of the curvatures of potential curves in the excited and ground states.

N	k	ΔE_k (eV)	M_k^0	$M_{k,Ja}^1$	z	$\sqrt{f_e/f_g}$
4	1	4.54	1.10	−0.21	1.04	1.03
	2	8.55	−0.24	−0.14	−0.26	1.24
10	1	2.72	2.07	0.48	0.85	0.91
	2	4.90	−0.70	0.21	0.18	1.02
20	1	1.99	−3.07	1.18	1.10	0.80
	2	3.03	1.47	0.27	0.30	1.06
50	1	1.62	4.15	1.72	[a]	[a]
	2	1.90	3.11	0.28	0.46	0.89
100	1	1.54	4.51	−1.57	0.76	0.72
	2	1.63	−4.08	0.78	0.48	0.84
120	1	1.53	4.56	−1.48	0.67	0.78
	2	1.59	−4.23	−0.83	0.47	0.85

[a]No minimum in the excited state potential energy along Q_{Ja}.

sideration of discrete states so we can apply Albrecht's theory. To avoid problems with an open shell electronic ground state, we restrict ourselves to rings where the number of atoms N equals $4n+2$. Because of the full periodicity of the dimers the relevant configurational space is two dimensional. The generalized coordinates are r_l and r_s, the two bond length in the unit cell, or equivalently,

$$r_+=(r_l+r_s)/2 \quad \text{and} \quad r_-=(r_l-r_s)/2 \ . \tag{31a}$$

Instead of r_- one can use the dimensionless dimerization parameter

$$x=r_-/B_\beta \ . \tag{31b}$$

From Fig. 5 it follows immediately that the displacement of the atoms in the Q_{Ja} mode is half the change of the bond length in absolute value

$$u=|\Delta r_l|/2=|\Delta r_s|/2=|\Delta r_-|/2=B_\beta dx \ . \tag{31c}$$

In order to calculate the vibrational properties the total electronic energy must be evaluated. It is proportional to N for long chains and thus diverges linearly in the limit of infinite long chains. The increase of the total energy during a normal mode vibration, however, does not

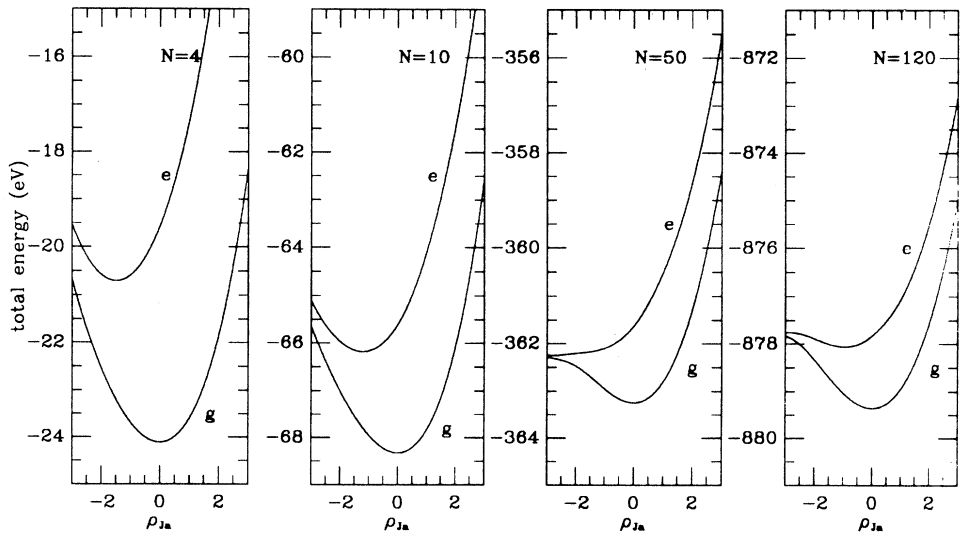

FIG. 6. Total energy curves for electronic ground state (g) and first excited state (e) as a function of the dimensionless Ja coordinate of the ground state, calculated by LHS model for various chains with length from $N=4$ to $N=120$.

diverge. For motions which correspond to one vibrational quantum it is, e.g., $\hbar\Omega$. Therefore the real amplitude of the change of a *bond* during vibration decreases with increasing N. As a matter of fact it is proportional to $1/\sqrt{N}$. The amplitude q_{Ja} of the *normal mode* Q_{Ja}, however, remains finite even for infinite chains. The change of ith bond length can be expressed as the product of the amplitude of the normal mode and the ith component of $Q_{Ja}=Q_{Ja}^{\rm cycl}$ normalized to one:

$$\Delta r_i = q_{Ja}(Q_{Ja})_i = q_{Ja}\frac{(-1)^i}{\sqrt{N}} . \tag{32}$$

Thus, the kinetic energy is

$$E_{\rm kin}=\sum_i \tfrac{1}{2}m_i\dot{u}_i^2=\sum_i \tfrac{1}{2}m\left[\frac{\Delta\dot{r}_i}{2}\right]^2=\tfrac{1}{2}m_{Ja}^{\rm red}\dot{q}_{Ja}^2 , \tag{33}$$

where $m_{Ja}^{\rm red}=m_{\rm CH}/4=5973$ a.u. is the reduced mass of the Q_{Ja} normal mode, independent from N. The potential energy in the harmonic approximation is $\frac{1}{2}f_{Ja}^{\rm red}(N)q_{Ja}^2$ with

$$f_{Ja}^{\rm red}(N)=\frac{d^2E_{\rm tot}}{dq_{Ja}^2}=\frac{1}{N}\frac{d^2E_{\rm tot}}{dr_-^2}=\frac{d^2\epsilon_{\rm tot}}{dr_-^2} , \tag{34}$$

where $\epsilon_{\rm tot}$ is the total ($\sigma+\pi$ electronic) energy per unit cell. This quantity remains finite and converges for N to infinity.

The π-electron energy eigenvalues and LCAO coefficients in the LHS model can be solved exactly for a cyclic chain which is therefore much simpler than the case of an open end chain, even for very large N. The latter can be solved only numerically. After straightforward algebra one obtains for the cyclic chain

$$\epsilon_{\pi,\rm tot}\equiv\frac{E_{\pi,\rm tot}}{4n+2}=-\frac{4t_0}{\pi}E\left[\frac{1}{\cosh x};n\right]\cosh x , \tag{35a}$$

$$\epsilon_{\sigma,\rm tot}\equiv\frac{E_{\sigma,\rm tot}}{4n+2}=-\frac{2t_0}{(R_1-R_2)}[B_\beta(\cosh x - x\sinh x)-(R_1-r_+)\cosh x] , \tag{35b}$$

where $t_0=A_\beta e^{(-r_+/B_\beta)}$ is the absolute value of the mean resonance integral. In Eq. (35a)

$$E\left[\frac{1}{\cosh x};n\right]=\frac{\pi}{4n+2}\sum_{j=-n}^{n}\left[1-\frac{1}{\cosh x}\sin^2 j\frac{\pi}{2n+1}\right]^{1/2} \tag{36a}$$

which can be regarded as a "finite elliptic sum" because in the limit $n\to\infty$ it converges exactly into the elliptic integral of the second kind.

The actual value of x (and r_+) can be obtained from the equilibrium conditions

$$\frac{\partial\epsilon_{\rm tot}}{\partial x}=0 \quad\text{and}\quad \frac{\partial\epsilon_{\rm tot}}{\partial r_+}=0 . \tag{37}$$

Equation (37) results in an equation for x of the form $x=f(x,n)$ with

$$f(x,n)=\frac{R_1-R_2}{B_\beta\pi}\sinh(2x)\left[K\left[\frac{1}{\cosh x};n\right]-E\left[\frac{1}{\cosh x};n\right]\right] . \tag{38}$$

Figure 7 illustrates the graphical solution of Eq. (38). The right-hand side of Eq. (38) depends on $N=4n+2$. For small n the only solution is $x=0$. For larger n the x_0 nonzero solution has a lower total energy than $x=0$. The x_0 value characterizing the dimerization saturates in the infinite limit. The gap opening due to dimerization has the value of $E_g=4t_0\sinh x_0$. The $f_{Ja}^{\rm red}(N)=f_{Ja}^{\sigma+\pi}$ force constant of the Q_{Ja} mode can also be obtained:

$$f_{Ja}^{\sigma+\pi}=\left.\frac{\partial^2\epsilon_{\rm tot}}{\partial r_-^2}\right|_{x=x_0}=\frac{4t_0}{\pi B_\beta^2}\cosh x_0\left\{\tanh^2 x_0\left[I\left[\frac{1}{\cosh x_0};n\right]-K\left[\frac{1}{\cosh x_0};n\right]\right]+\frac{B_\beta\pi}{2(R_1-R_2)}\left[1-\frac{2x_0}{\sinh(2x_0)}\right]\right\} . \tag{39a}$$

In Eq. (39a) K and I are "finite elliptical sums" of the first and third kinds similar to Eq. (36a):

$$K\left[\frac{1}{\cosh x};n\right]=\frac{\pi}{4n+2}\sum_{j=-n}^{n}\left[1-\frac{1}{\cosh^2 x}\sin^2 j\frac{\pi}{2n+1}\right]^{-1/2} , \tag{36b}$$

$$I\left[\frac{1}{\cosh x};n\right]=\frac{\pi}{4n+2}\sum_{j=-n}^{n}\left[1-\frac{1}{\cosh^2 x}\sin^2 j\frac{\pi}{2n+1}\right]^{-3/2} . \tag{36c}$$

Using for A_β, B_β, R_1, and R_2 the values discussed in Sec. III A one obtains from solving Eqs. (38) and (39a) in

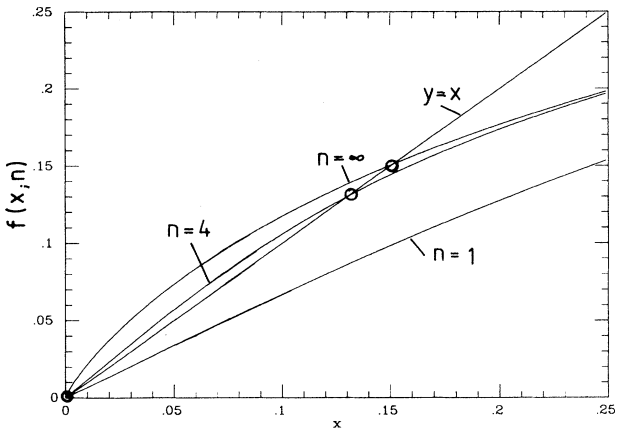

FIG. 7. Graphical solution of Eq. (38) for three different chain lengths. Solutions are indicated by open circles. There is no bond alternation for a cyclic chain with 6 atoms ($n=1$) whereas for $N\rightarrow\infty$ the bond alternation saturates. With parameters mentioned in Sec. III A this corresponds to $r_l-r_s=0.09$ Å.

the infinite limit: $x_0(n\rightarrow\infty)=0.1511$, $r_+(n\rightarrow\infty)=1.409$ Å, and $f_{Ja}^{\sigma+\pi}(n\rightarrow\infty)=5.390$ mdyn/Å. Because in the AMM the "bare" system without π electrons plays an important role it is worth to compare the latter force constant value with that of a "bare" σ-force constant:

$$f_{Ja}^{\sigma}=\left.\frac{\partial^2\epsilon_{\sigma,\mathrm{tot}}}{\partial r_-^2}\right|_{x=0}=\frac{2A_\beta e^{-R_1/B_\beta}}{(R_1-R_2)B_\beta}=8.071\ \mathrm{mdyn/Å} \tag{39b}$$

which is of course independent from N.

For evaluating the Albrecht's A, B terms the electronic dipole matrix elements and the FC integrals must be computed. For the former this can be done straightforwardly inserting the proper LCAO coefficients into Eq. (27). Since every energy level is double degenerate due to $4n+2$ symmetry the matrix element is the interference of four terms according to Fig. 8.

The FC integrals are very simple as compared with the case of short chains. As it was mentioned earlier [see Eq. (34)] the derivatives of the total energy with respect to the normal coordinate amplitude q_{Ja} are needed which is the derivative with respect to r_- divided by $\sqrt{N}$. The difference between the total energy in the ground and excited states is finite because only one electron is excited, therefore all derivatives with respect to q_{Ja} are equal in the ground and excited states in the infinite limit. For this reason the *delocalized* normal mode wave functions are identical in the ground and excited states and we arrive at the solid state limit. The FC integrals are then immediately obtained for $z=0$ as

$$\langle\{v\}^e|\{i\}^g\rangle\equiv\delta_{\{v\},\{i\}}\ . \tag{40}$$

As a consequence of Eq. (40) the A term in Eqs. (17) vanishes. Furthermore in the B term [Eq. (17c)] the product of matrix elements is nonzero only if the vibronic excited state is identical either with the initial ($v=0$) or with the final ($v=1$) vibronic state as it is illustrated on Fig. 9. The former corresponds to the incoming resonance the latter to the outgoing resonance. After straightforward calculations the following expression for the transition polarizability related to one unit cell can be obtained:

$$\alpha=\frac{1}{2\pi\sqrt{2\Omega}}\int_{\sinh x_0}^{\cosh x_0}dy\,\frac{y\rho(y)}{\sqrt{y^2-\sinh^2x_0}\sqrt{\cosh^2x_0-y^2}}\left[\frac{1}{4t_0y-\omega_L+i\Gamma}+\frac{1}{4t_0y+\Omega-\omega_L+i\Gamma}\right],$$
$$\rho(y)\equiv r_+-r_-+\frac{16}{B_\beta}r_+^2e^{-2x_0}\left[1+\frac{8\sinh(2x_0)}{y^2}\right]\frac{1}{y^2}\ . \tag{41}$$

In Eq. (41) ω_L is the quantum energy of the exciting laser, Ω is the frequency of the Q_{Ja} normal mode, and Γ is a damping factor. The prefactor in the integrand diverges for HOMO-LUMO ($y=\sinh x_0$) excitation and for excitation from the bottom of the HOMO band to the top of the LUMO band ($y=\cosh x_0$). The latter occurs at much higher quantum energies as usually used for resonance excitation and therefore does not play any role. Figure 10 shows the excitation profiles calculated from Eq. (41) for various damping factors Γ. The two peaks with a

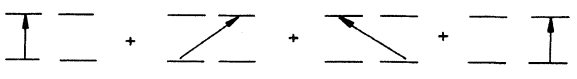

FIG. 8. Schematic representation of the four degenerate one-electron transitions of a cyclic chain with $4n+2$ atoms.

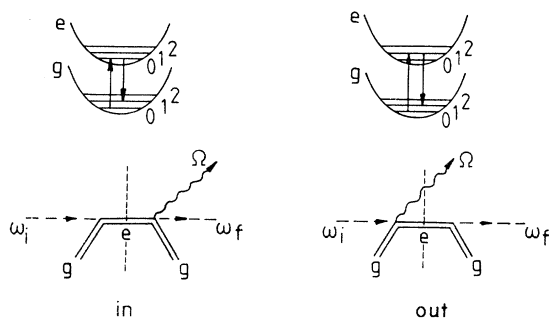

FIG. 9. Diagrams corresponding to the two terms in the Raman cross section of the infinite long linear chain [see Eq. (41)]. $v_g=0\rightarrow v_e=0\rightarrow v_g=1$ describes incoming resonance and $v_g=0\rightarrow v_e=1\rightarrow v_g=1$ describes outgoing resonance.

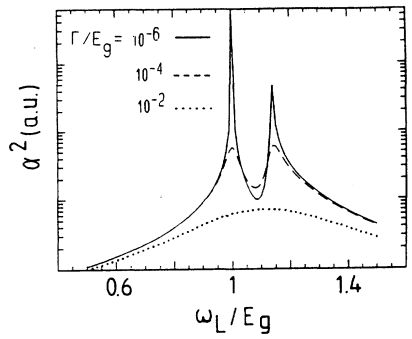

FIG. 10. Resonance Raman excitation profile for an infinite long linear chain calculated by generalized CLM using LHS model [Eq. (41)].

difference equal to Ω/E_g corresponds to the incoming and outgoing resonances.

IV. COMPARISON OF THE EXPLICIT RESULTS OF ALBRECHT'S APPROXIMATION FOR THE LHS MODEL TO THE CURRENT MODELS

In the following we compare the results of Albrecht's theory for resonant Raman effect in strictly one-dimensional chains described by LHS model with that of AMM, ECCM, and conventional CLM.

A. Comparison to the amplitude mode model (AMM)

The AMM is a solid-state approximation. Figure 11(a) shows the diagram for a Raman process in the solid-state limit. An incoming photon with wave number q and energy ω_i creates an electron-hole pair which—after emitting a phonon with wave number k and energy Ω—recombine to a photon with wave number $q-k$ and energy ω_f. The phonon propagator $D(\Omega)$ is considered to be renormalized from a "bare" phonon propagator $D_0(\Omega)$ which describes vibrations without π electrons via strong electron-phonon coupling according to Fig. 11(b). $\Pi(\Omega)$ is the polarization bubble which includes electronic interactions. $D_0(\Omega)$ can be obtained from the Fourier transform of the equation of motion of a damped harmonic oscillator. Allowing many modes to be coupled with the π electrons the "bare" phonon propagator is

$$D_0(\Omega)=\sum_n \left[\frac{\lambda_n}{\lambda}\right]\frac{(\Omega_n^0)^2}{\Omega^2-(\Omega_n^0)^2-i\Omega\delta_n}\ , \tag{42}$$

where $\lambda=\sum_n \lambda_n$. For *trans*-polyacetylene, e.g., there are two modes with considerable electron-phonon coupling constant λ_n. The renormalized phonon propagator $D(\Omega)$ is according to Fig. 11(b)

$$D(\Omega)=\frac{\tilde{D}_0(\Omega)}{1-\Pi(\Omega)\tilde{D}_0(\Omega)}\ , \tag{43}$$

where $\tilde{D}_0(\Omega)=[2\lambda/N(0)]D_0(\Omega)$, $N(0)$ is the electron density of states at the Fermi level of the "bare" system, before renormalization.

For a Peierls chain the dependence of the polarization bubble on Ω can be neglected if $\Omega \ll E_g$. This is called in the AMM as the adiabatic approximation.[21] Thus $\Pi(\Omega)$ can be replaced by $\Pi(0)$. The "bare" phonon frequencies (Ω_n^0) are the poles of $D_0(\Omega)$ while the renormalized frequencies (Ω_n^R) are the poles of $D(\Omega)$. The latter are determined by the roots of the denominator that is, where $1-\Pi(0)\tilde{D}_0(\Omega)=0$ holds. This is a polynomial equation for Ω^2 which can be written in the form $\prod\{[\Omega^2-(\Omega_n^R)^2]/[\Omega^2-(\Omega_n^0)^2]\}=0$. Taking these two expressions at $\Omega=0$ and using $D_0(0)\equiv -1$ from Eq. (42), the product rule follows immediately:

$$2\tilde{\lambda}:=1+\Pi(0)\frac{2\lambda}{N(0)}=\prod_n\left[\frac{\Omega_n^R}{\Omega_n^0}\right]^2 . \tag{44}$$

The effective electron-phonon coupling constant $\tilde{\lambda}$ defined by Eq. (44) is the central parameter in the AMM. From Eqs. (43) and (44) it follows that for a given $\tilde{\lambda}$ the position of the Raman line can be obtained from the equation $D_0(\Omega)=-1/(1-2\tilde{\lambda})$ $(2\tilde{\lambda}<1)$. The solution is illustrated graphically on Fig. 12. In our simplified case there is only one contribution to the sum in Eq. (42) and to the product rule. Remaining in this model Eq. (44) gives the possibility to compute $\tilde{\lambda}$ explicitly by means of the LHS model by comparing the Q_{Ja} normal mode frequency obtained for the total $\sigma+\pi$ electronic system (Ω^R) with the frequency for the same system but without π electrons (Ω^0). In the AMM the chain is infinite long. $\tilde{\lambda}$ of the infinite long Peierls chain can be calculated exactly using Eqs. (39a) and (39b) with $n\to\infty$ in the former. The parametrization of LHS described in Sec. III A results in $2\tilde{\lambda}(\infty)=f_{Ja}^{\sigma+\pi}(n\to\infty)/f_{Ja}^{\sigma}=0.6678$.

We stress however, that it is possible to define $\tilde{\lambda}$ for finite chains as well. Using Eq. (44) we can compute $\tilde{\lambda}$ as a function of the chain length. These calculations have to be carried out for open end chains and not for chains with periodic boundary conditions. The behavior of

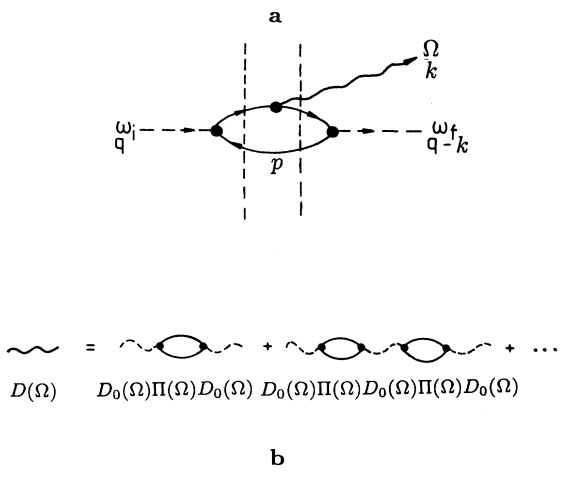

FIG. 11. Raman process in the AMM (a) and renormalized phonon propagator (b).

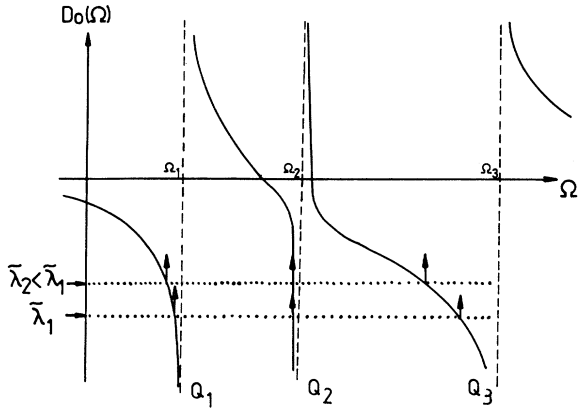

FIG. 12. Graphical solution of $D_0(\Omega)=-1/(1-2\tilde{\lambda})$ for determination of the Raman-line positions in the AMM.

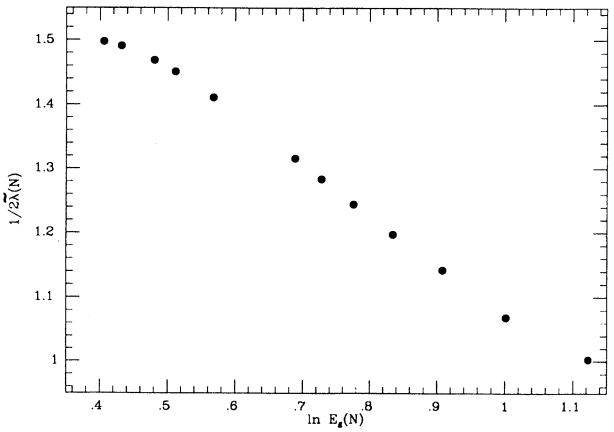

FIG. 14. Inverse of $2\tilde{\lambda}$ vs. logarithm of gap energy for increasing chain length N for the AMM. All quantities were calculated by generalized CLM using the LHS model.

chains and rings is opposite to each other with respect to the frequency response as it can be shown by solving Eq. (30) numerically for chains and calculating Eqs. (39) for rings (see Fig. 13). This result can be qualitatively interpreted as follows. f_{Ja}^{σ} from Eq. (39b) is the same for chains and rings independent from their length, that is, $\tilde{\lambda}$ is proportional to the curvature of the total renormalized $(\sigma+\pi)$ electronic energy which is correlated with the amount of bond length alternation. The latter increases with increasing N for chains with cyclic boundary conditions as is immediately realized from the lack of any bond alternation in the benzene ring but decreases with increasing N for open end chains. The infinite limit is of course the same. This means, one should be careful with cyclic boundary condition for finite systems in general.

In analyzing RR experiments by means of the AMM the plot of $\tilde{\lambda}$ versus $\ln E_g$ plays an important role. Choosing $\tilde{\lambda}$ as proportional to the product of the square of the experimentally measured Raman line positions of the satellite peaks and E_g as proportional to the frequency of the exciting laser results in a nearly straight line for $\tilde{\lambda}^{-1}$ versus $\ln E_g$.[22] Carrying out the same plot for finite chains, calculating $\tilde{\lambda}(N)$ and $E_g(N)$ with LHS model results in Fig. 14. This curve is also nearly a straight line in a broad interval. This is the reason why the AMM works well as far as the *positions* of the Raman lines are concerned.

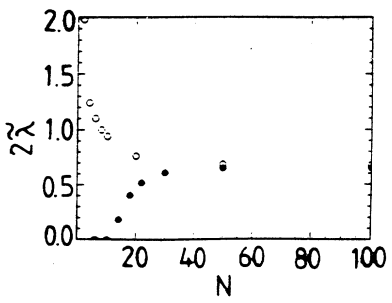

FIG. 13. Chain length dependence of $\tilde{\lambda}$ calculated by generalized CLM using LHS model for open end chains (○) and for chains with cyclic boundary conditions (●).

To compare our result for the RR *intensity* [Eq. (41)] with the excitation profile obtained from AMM the Raman cross section for a Peierls chain was computed by the AMM and according to LHS model. In the former electrons were considered in the neighborhood of the Fermi points $\pm p_F$ of the "bare," undimerized (metallic) chain by approximating their $\varepsilon(p)$ dispersion with a linear relationship. In addition the approximation $\Omega \ll E_g$ was used in all formulas, not only for $\Pi(\Omega)$.[21] This yielded for the RR intensity

$$\frac{I}{I_0} \propto N(0)\frac{\lambda}{E_g^2}\left|f\left[\frac{\omega_L}{E_g}\right]\right|^2 \mathrm{Im}D(\Omega) \ . \tag{45}$$

$D(\Omega)$ is the same as in Eq. (43) and describes the position of the Raman line(s). The $f(x)=f(\omega_L/E_g)$ resonance factor contains the dependence on laser excitation frequency and has the form shown in Fig. 15. It has a maximum if $\omega_L=E_g$ and its half width depends on the damping factor Γ. For $\Gamma\to 0$ $f(x)$ diverges at $x=1$. This result has to be compared with Fig. 10. It is evident that there is one peak missing in the AMM. Both tree-type diagrams illustrated in Fig. 9 lead to the same loop diagram which is seen in Fig. 11(a) in the solid-state limit. The diagram in Fig. 11(a) should have two terms differing in Ω/E_g, depending on where we cut the diagram [dashed lines in Fig. 11(a)]. The reason for the lack of two distinct peaks is the approximation $\Omega/E_g \ll 1$. Without this approximation $f(x)$ would really have two peaks as it can be seen from Eq. (A2.4) of Ref. 21.

In the experimental results on *trans*-polyacetylene there is only one broad peak in the excitation profile even for the part of the Raman line which characterizes the long segments.[53] This can have two reasons. First, if the electronic damping factor is greater than 1% of the gap E_g the two peaks smear out into one broad peak (see Fig. 10). Indeed, for fitting experimental curves with AMM a Γ (or equivalently a three-dimensional cutoff) value has to

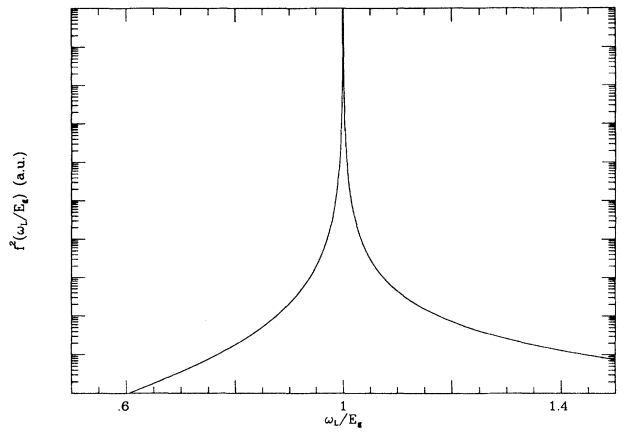

FIG. 15. Resonance Raman excitation profile proportional to the square of $f(\omega_L/E_g)$ calculated by the AMM for a Peierls chain (see Ref. 21).

be used which amounts to 10% of the E_g.[22] As a second reason, the real polymers are inhomogeneous so the distribution of E_g and Ω will smear the two peaks as well. The second effect is most likely dominant.

The AMM has the advantage to treat various RR modes simultaneously and to provide a simple technique to obtain vibrational frequencies and relative intensities of RR bands. From a comparison of Figs. 10 and 15 it is evident that the resonance effect for a given chain is reproduced as a limiting case of a molecular physics model in the form of the LHS approximation. However, the AMM has the disadvantage, that the analysis needs two fitting parameters per mode which will result in $2n$ parameters for n modes. This number can be reduced by one if the product rule is considered. In addition, for the quantitative analysis of the dispersive line shape of a given RR-mode problems arise. First of all it is assumed in the AMM that all chains in a sample are infinite translationally symmetric, for which the solid-state limit is valid. In real polymers it seems to be more realistic that there are several short conjugations for which this assumption is not valid. Assuming that all chains are perfect and infinite but have various $\tilde{\lambda}$ seems also unrealistic from a microscopic point of view, and can be accepted only phenomenologically. Of course a distribution in $\tilde{\lambda}$ leads to a distribution in both the energy gap and the phonon frequency. Thus, it is formally possible to describe dispersive RR line shapes. Another serious problem is that in AMM the resonance effect $f(x=1)$ is assumed to be constant and independent from the excitation energy or from $\tilde{\lambda}$. This is not justified from any experimental or theoretical consideration in particular not for finite conjugation lengths. On the contrary: explicit calculations on the Hückel level show the opposite behavior.[30] For long chains a $1/E^2$ dependence of the matrix elements on the excitation energy was found. A similar behavior for various short chains is shown in Table III in this paper. The change of E_g^2 in the denominator of Eq. (45) is not enough to describe the resonance, in particular because the transition matrix elements enter with the fourth power. Thus their influence is very dramatic. Accordingly a quantitative analysis of the RR line shapes from a simple AMM can lead to an incorrect distribution function of $\tilde{\lambda}$. In a generalized form with two peaks in the excitation profile the AMM approaches the generalized CLM. The distribution in $\tilde{\lambda}$ *can* then be explained on a microscopic level as a consequence of a distribution in chain lengths (Fig. 13).

B. Comparison to the effective conjugation coordinate model (ECCM)

The ECCM considers chains with quasifinite conjugation length as obtained from periodic boundary conditions. The central parameter is an effective conjugation coordinate (*Ja* coordinate) as described already in Sec. III A. Accordingly, *Ja* is a heuristically constructed internal coordinate for an optimum characterization of the strong coupling between the molecular geometry and the π electrons of a conjugated polymer. In general it can be constructed from the bond alternation coordinate of the backbone. $\sum_i (-1)^i r_i$, where i runs over all bonds of the backbone in the unit cell. The purpose for the construction of this mode was the intention to give a microscopic interpretation to the parameter $\tilde{\lambda}$ in the amplitude mode model.[23] $\tilde{\lambda}$ was replaced by an effective force constant f_{Ja}, which is the force constant of the *Ja* mode. Different values for f_{Ja} lead to different normal frequencies and different normal modes. The various f_{Ja} correspond to various lengths of conjugation. f_{Ja} decreases with increasing conjugation length. For computing the change of normal frequencies and normal modes with f_{Ja}, a simplified *GF* formalism can be used. Instead of considering the whole inverse kinetic (G) and force constant (F) matrix only the blocks with dimension equal to the relevant number of normal modes (experimentally observed resonantly enhanced Raman modes) are considered. These blocks have, e.g., the dimension 2 (at most 3) for real *trans*-polyacetylene. Furthermore the dependence on conjugation length is taken into account for only one element in the F matrix, namely, the f_{Ja}. The *Ja* mode in the ECCM is the translationally symmetrical extension of the eigenvector of the relevant *GF* block (with strongest coupling with π electrons) if replacing $f_{Ja}(N\rightarrow\infty)$ into the F matrix. For other values of f_{Ja} the eigenvalues change and the modes mix if the dimension of the reduced matrices is >1. In this case Q_{Ja} is not a normal mode in general. Figure 16 illustrates the relation between f_{Ja} and normal mode frequency Ω for the case of two RR modes. For the strictly linear and infinitely long chain there is only one RR mode. Thus, the relevant G and F blocks are one dimensional and instead of two there is only one curve which is shown as dashed line in Fig. 16. This mode is then always the *Ja* mode with different frequencies for different values of f_{Ja}.

In the ECCM the assumption is used that the Raman intensity of a mode is proportional to the *Ja* content of that mode which can be regarded as the "coupling strength" of the mode to the π electrons. This is a good approximation for comparing Raman intensities, and also IR oscillator strengths, of various modes on the same

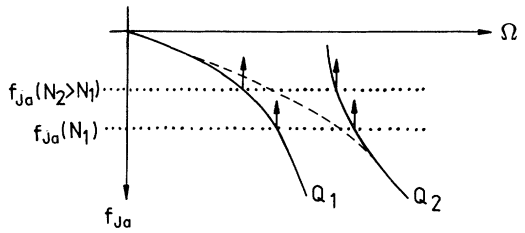

FIG. 16. Graphical determination of the Raman-line positions as a function of the effective force constant f_{Ja} in the ECCM. The relative weight of Q_{Ja} in the normal modes changes if there are more than one Raman active modes.

chain. However, it does not take into account the role of electronic transition matrix elements in the resonance Raman process. In the strictly one-dimensional bond alternating chain with only one mode the ECCM yields a constant Raman intensity. This result is not correct because the transition matrix elements depend strongly on the transition energy and thus on the conjugation length. Thus, similar to the AMM line shapes of dispersive modes cannot be analyzed within the ECCM.

The dependence of the positions of the Raman lines on conjugation length is described by ECCM only qualitatively. The reason for this is that it uses cyclic boundary conditions and thus does not take into account finite chain effects. As a matter of fact the effective force constant f_{Ja} for the Ja mode in a finite chain is derived from an infinite chain by considering a finite interaction width of the local force constants according to the relation

$$f_{Ja}^{\mathrm{ECCM}}(N_{\max}) := \tfrac{1}{2}(f_{11}^{(0)}+f_{22}^{(0)})-2f_{12}^{(0)} + \sum_{n=1}^{N_{\max}} (f_{11}^{(n)}+f_{22}^{(n)}-2f_{12}^{(n)}) . \quad (46)$$

in Eq. (46) f_{11}, f_{22}, and f_{12} are the C—C, $C=C$ stretching constants and (C—C)-($C=C$) interaction respectively. The upper index (n) refers to the number of unit cells between corresponding bonds. It should be mentioned, that the real length (N) of a finite chain described by ECCM with Eq. (46) can be approximately expressed as $N=4(N_{\max}+1)$, because $n=0$ corresponds already to butadiene and increasing $N_{\max}$ by 1 means increasing the chain length by one unit cell in both directions. As it is known the interaction force constant $f_{(12)}^{(n)}$ is always positive and the diagonal force constants between different unit cells $f_{(11)}^{(n)}$, $f_{(22)}^{(n)}(n>0)$ are negative. They quickly decrease with increasing distance. Consequently, f_{Ja} decreases and "saturates" with increasing $N_{\max}$ and thus yields a formally proper dependence of the normal mode frequencies on chain length as it can be seen in Fig. 16. However this description is only qualitatively correct as it can be shown for the example of the strictly one-dimensional chain using the LHS model. As it was mentioned in Sec. III A the LHS model is capable for calculating force constants. Table IV illustrates the quality of this comparing bond lengths and force constants as obtained from the LHS model and from *ab initio* calculation for butadiene.[54] We stress that we did not try to scale the force constants, because we were not interested in the absolute values but in the changes as a function of the chain length. For calculating f_{Ja}^{ECCM} with Eq. (46) one needs the $f_{ij}^{(n)}$ values. Extending the calculations to long chains shows that the force constants in the center part of a chain with 100 atoms already equal those for the infinite chain. This means that there is a quasitranslational symmetry for the force constants at the center. Table V shows the $f_{ij}^{(n)}$ values from the center of a chain with 100 atoms for various values of n within the LHS model. The corresponding f_{Ja}^{ECCM} effective force constant values calculated by Eq. (46) using these $f_{ij}^{(n)}$'s are shown in the first row of Table VI.

In addition, in the LHS model it is possible to carry out the normal coordinate analysis with *GF* method not only for the small block, assuming translational symmetry as in the ECCM but for the whole $(N-1)\times(N-1)$ dimensional matrices as they were defined by Eqs. (28)–(30). This can be done for the system including the π electrons as well as for the system described only by the σ part of the LHS Hamiltonian. For each chain length the Q_{Ja} normal mode can be obtained as it was mentioned in Sec. III A. To compare the results with the ECCM one has to compute the expectation values of the force constant matrix with respect to the Q_{Ja} unit vector. This reduced force constant is

$$f_{Ja}^{\mathrm{CLM}}(N)=f_{Ja}^{\mathrm{red}}(N) := \mathbf{Q}_{Ja}(N)\hat{F}(N)\mathbf{Q}_{Ja}(N) . \quad (47a)$$

Similarly one can define the reduced mass as

$$m_{Ja}^{\mathrm{CLM}}(N)=m_{Ja}^{\mathrm{red}}(N) := \mathbf{Q}_{Ja}(N)\hat{G}^{-1}(N)\mathbf{Q}_{Ja}(N) . \quad (47b)$$

Table VI shows also these reduced values for chains with 4, 8, 20, 50, and 100 atoms both for $\sigma+\pi$ (renormalized) and for only σ (bare) systems. The frequencies are eigenvalues of the *GF* matrix. As can be checked immediately the relation $\Omega^2=f/m$ between the corresponding values still holds. It is also seen from Table VI that the various values obtained for open end chains with increasing length converge to the infinite limits obtained with cyclic boundary conditions. The effect of the change of m_{Ja}^{red} with N is most clearly seen for the set of bare values. In this case only σ-force constants between neighboring

TABLE IV. Comparison of the bond lengths and the force constants of butadiene calculated by *ab initio* method (Ref. 54) and by our LHS method. (All force constants are in mdyn/Å.)

	r_1(Å)	r_2(Å)	$f_{11}^{(0)}$	$f_{22}^{(0)}$	$f_{12}^{(0)}$	$f_{22}^{(1)}$
ab initio	1.457	1.339	5.608	9.549	0.461	−0.136
LHS	1.476	1.340	8.063	14.992	0.943	−0.471

TABLE V. Force constant values (all in mdyn/Å) taken from the middle part of a chain with 100 atoms, calculated by LHS model (n is the distance between bonds measured in unit cells).

n	$f_{11}^{(n)}$	$f_{22}^{(n)}$	$f_{12}^{(n)}$
0	8.1783	12.8471	1.3947
1	−0.3971	−0.7267	0.2568
2	−0.1010	−0.1848	0.0774
3	−0.0339	−0.0621	0.0280
4	−0.0129	−0.0237	0.0111
5	−0.0053	−0.0097	0.0047
10	−0.0001	−0.0002	0.0001
15	−0.0000	−0.0000	0.0000

atoms exist and they all are identical. The f_{Ja}^{σ} force constant is therefore independent from chain length. In contrast the vibronic frequency Ω_{Ja}^{σ} changes with N corresponding to a change of m_{Ja}^{σ} with N. The main point is however, that comparing the corresponding f_{Ja}^{ECCM} and f_{Ja}^{CLM} values in Table VI shows that the effective Ja force constant f_{Ja}^{ECCM} leads to a qualitatively correct but quantitatively an incorrect dependence on chain length.

C. Comparison to the conventional conjugation length model (CLM)

The CLM was discussed already to some extent in Sec. III. It assumes that there are various conjugation lengths in a conjugated polymer due to interruption of conjugation by conformational and chemical defects. There is thus a distribution in the lengths of segments with perfect conjugation between defects. In the conjugation length model this is transformed into a distribution of finite chain lengths. The strength of the interruption of a chain by a defect can be characterized by its interruption parameter η defined as

$$\eta := \frac{\Delta E_{\mathrm{def}}}{\Delta E_{\mathrm{cut}}} . \tag{48}$$

Here ΔE_{def} and ΔE_{cut} describe the increase of the first excitation energy of a chain due to a given defect or due to a cut of the chain at the same site, respectively.[13] The calculated value for η depends to some extent on the length of the chain and on the location of the defect. For sp^3 and sp^3+ carbonyl defects, e.g., it is between 70–90 %. In the CLM always 100% interruption is assumed. It describes the RR bands by the A term alone. For the chain length dependence of the electronic parameters, transition energies, and matrix elements, the results of Hückel calculations are used and the vibronic overlaps are treated within the FC approximation. Thus the CLM is the only model among the three investigated in this paper which really considers finite conjugation lengths with no translational symmetry and no cyclic boundary conditions on the one hand and explicit electronic dipole matrix elements on the other. One disadvantage of the model originates from the use of extrapolated experimental values for the chain length dependence of the vibronic parameters like frequencies and FC constants. Nevertheless, using these parameters the frequency shifts with chain length can be obtained with a similar diagram as in the case of the AMM (Fig. 12) and ECCM (Fig. 16). This is demonstrated in Fig. 17 where the third quadrant expresses the resonance condition, the second quadrant the relation between energy gap and chain length, and the first quadrant the relation to the vibrational frequency for two different modes.

With a proper distribution function of the conjugation length the RR line shapes can be well fitted for all laser excitations between 400 and 670 nm. The distribution function may be bimodal characterizing the ordered and disordered parts of the polymer.[19,6] The change of the RR line shape in experiments where defects are induced artificially on conjugated polymer chains[8,11] or during *in situ* electrochemical doping[55] can be analyzed successfully with CLM.

In addition to the nonsatisfactory treatment of vibronic contributions several other problems arise with CLM. First, in the CLM the Albrecht B term is neglected. This term is, however, important for very long chains, as it was discussed earlier. However, if the typical length of undisturbed conjugation is shorter than several ten carbon atoms, neglecting B as compared to A is a good approximation, since the shift between potential curves in the ground and excited states is large and thus enhances the A term over the B term. Also, the dipole matrix element which enters into A is larger than its first derivative which enters into B. Another problem results from the lack of the minimum in the excited state potential for a certain range of chain lengths as it was discussed in Sec. III B. As a consequence a conventional FC analysis cannot be carried out for medium long linear chains. As it was pointed out, the reason for this may be the strong

TABLE VI. f_{Ja}^{ECCM} as calculated by LHS model using Eq. (46) with $N=4(N_{\max}+1)$ (see text) and the expectation values of the force constant ($\hat{F}$) and inverse mass ($\hat{G}^{-1}$) matrices for finite chain length (N) with respect to the Q_{Ja} mode together with the eigenfrequencies of the same mode as calculated by the LHS model using Eqs. (47) and (30), with and without π electrons.

N	4	8	20	50	100	∞
f_{Ja}^{ECCM}(mdyn/Å)	7.723	6.086	5.434	5.391	5.391	5.390
$f_{Ja}^{\mathrm{CLM}} \equiv f_{Ja}^{\sigma+\pi}$(mdyn/Å)	10.301	8.696	6.143	5.496	5.413	5.390
f_{Ja}^{σ}(mdyn/Å)	8.071	8.071	8.071	8.071	8.071	8.071
$m_{Ja}^{\sigma+\pi}$(a.u.)	7223	6717	6019	5980	5975	5973
m_{Ja}^{σ}(a.u.)	7071	6217	6010	5979	5974	5973
$\Omega_{Ja}^{\sigma+\pi}$(cm^{-1})	2099	2000	1776	1685	1673	1669.7
Ω_{Ja}^{σ}(cm^{-1})	1878	2003	2037	2042	2043	2043.2

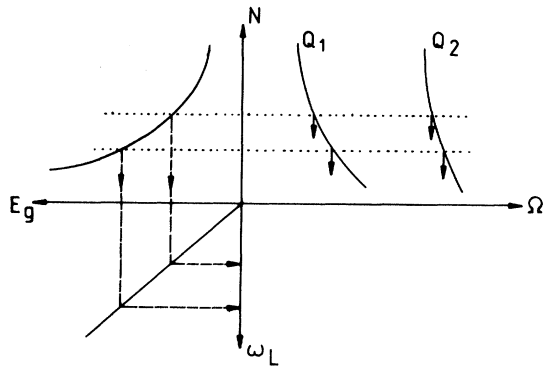

FIG. 17. Relation between laser energy ω_L, gap energy E_g, chain length N, and vibrational frequency Ω in the CLM. The dotted and dashed lines refer to two different laser energies.

perturbing role of the soliton configuration on the excited state energy hypersurface. Thus, this problem exists only for polymers with a degenerate ground state like, e.g., *trans*-polyacetylene. This problem may not be relevant even for *trans*-polyacetylene if one of the following statements are true.

(A) Solitons are not excited due to three-dimensional interactions as it was argued by several authors.[56]

(B) The contribution from chains for which the FC problem exists is not important, because most chains in the sample are either shorter or longer than the critical lengths. It should be pointed out that although the critical length from our calculations is in the region from several tens to around a hundred, these values are parameter dependent. However, within the present approach for a chain with degenerate ground state there definitely exists a critical interval for the application of FC theory. This problem is very general and concerns also the other models, in particular the ECCM.

V. DISCUSSION AND CONCLUSION

The final problem to be discussed refers to the question which model is closest to the real polymer? There is enough experimental and theoretical evidence that defects limit conjugation in conjugated polymers. A defect limited conjugation has, e.g., a bond length distribution comparable to a finite chain.[57] The AMM and the ECCM consider infinite chains—explicitly or implicitly—assuming translational symmetry or cyclic boundary conditions. This can lead to quantitative or even qualitative errors. In contrast, the CLM especially in its extended version presented in this paper considers real finite, open end chains. From this point of view the CLM is closest to experiments and will match the conditions of the polymer in an optimum way.

Summarizing, the three models—amplitude mode model (AMM), effective conjugation coordinate model (ECCM), and conjugation length model (CLM)—were compared with each other for the case of a strictly one-dimensional bond alternating chain of finite or infinite length as described by the Longuet-Higgins–Salem approximation.

It was shown that for a simplified consideration, mainly for analysis of the position and relative intensities of the resonance Raman lines, both AMM and ECCM are appropriate even though they do not consider a realistic structure of the chains. For a detailed description and in particular for a description of dispersive Raman modes an explicit consideration of the conjugation length is needed including the evaluation of the matrix elements, transition energies, and force constants. The model which fulfills this requirements is the conjugation length model in its extended version. It was shown that the excitation profile calculated with Albrecht's theory and LHS approximation in the quasi-infinite limit results in a resonance shape similar to the results of AMM for a Peierls chain. The correct calculation for the transition polarizability results in two peaks, one for incoming and one for outgoing resonances, respectively.

Finally, it was shown that the usual FC analysis is not appropriate for medium long linear chains because of the dramatic difference in the shape of the total energy hypersurface for ground and excited states. This is due to the strong and very complicated effect of electron excitation on the geometry of the oligomer. It may be worth investigating theoretically the FC problem with more sophisticated methods for oligomers, varying their length in a broad range.

ACKNOWLEDGMENTS

The authors gratefully acknowledge valuable discussions with A. Karpfen, M. Kertész, B. Kohler, P. Surján, P. Szalay, and A. Zawadowsky. The work was supported by the Fonds zur Förderung der wissenschaftlichen Forschung in Austria, the Bundesministerium für Wissenschaft und Forschung in Austria and Grant No. 64/1987 in Hungary.

[1]S. Lefrant, L. S. Lichtmann, H. Temkin, and D. B. Fitchen, Solid State Commun. **29**, 191 (1979).
[2]H. Kuzmany, Phys. Status Solidi B **97**, 521 (1980).
[3]I. Harada, Y. Furukawa, M. Tasumi, H. Shirakawa, and S. Ikeda, J. Chem. Phys. **73**, 4746 (1980).
[4]L. S. Lichtmann, A. Sarhangi, and D. B. Fitchen, Chem. Scr. **17**, 149 (1981).
[5]Z. Vardeny, E. Ehrenfreund, O. Brafman, and B. Horovitz, Phys. Rev. Lett. **51**, 2326 (1983).
[6]H. Kuzmany, Pure Appl. Chem. **57**, 235 (1985).
[7]I. Harada, Y. Furukawa, T. Arakawa, H. Takeuchi, and H. Shirakawa, Mol. Cryst. Liq. Cryst. **117**, 335 (1985).
[8]P. Knoll and H. Kuzmany, Mol. Cryst. Liq. Cryst. **106**, 317 (1984).
[9]M. A. Schen, S. Lefrant, E. Perrin, J. C. W. Chien, and E. Mulazzi, Synth. Met. **28**, D287 (1989).
[10]A. Pron, E. Faulques, and S. Lefrant, Polym. Commun. **28**, 27 (1987).

[11]H. Kuzmany and J. Kürti, Synth. Met. **21**, 95 (1987).
[12]R. Zemach, Z. Vardeny, O. Brafman, E. Ehrenfreund, A. J. Epstein, R. J. Weagley, and H. W. Gibson, Mol. Cryst. Liq. Cryst. **118**, 423 (1985).
[13]J. Kürti and H. Kuzmany, in *Electronic Properties of Conjugated Polymers,* edited by H. Kuzmany, M. Mehring, and S. Roth (Springer-Verlag, Berlin, 1987), p. 43.
[14]W. Wallnöfer, E. Faulques, H. Kuzmany, and K. Eichinger, Synth. Met. **28**, C533 (1989).
[15]E. P. Steigmeier, H. Anderset, W. Kobel, and D. Baeriswyl, Synth. Met. **18**, 219 (1987).
[16]T. Danno, J. Kürti, and H. Kuzmany, Phys. Rev. B **43**, 4809 (1991).
[17]H. Kuzmany, J. F. Rabolt, B. L. Farmer, and R. D. Miller, J. Chem. Phys. **85**, 7413 (1986).
[18]H. Kuzmany, E. A. Imhoff, D. B. Fitchen, and A. Sarhangi, Phys. Rev. B **26**, 7109 (1982).
[19]G. P. Brivio and E. Mulazzi, Chem. Phys. Lett. **95**, 555 (1983).
[20]B. Horovitz, Solid State Commun. **41**, 729 (1982).
[21]B. Horovitz, Z. Vardeny, E. Ehrenfreund, and O. Brafman, J. Phys. C **19**, 7291 (1986).
[22]E. Ehrenfreund, Z. Vardeny, O. Brafman, and B. Horovitz, Phys. Rev. B **36**, 1535 (1987).
[23]C. Castiglioni, J. T. Lopez Navarrete, G. Zerbi, and M. Gussoni, Solid State Commun. **65**, 625 (1988).
[24]G. Zerbi, C. Castiglioni, J. T. Lopez Navarrete, T. Bogang, and M. Gussoni, Synth. Met. **28**, D359 (1989).
[25]J. T. Lopez Navarrete, B. Tian, and G. Zerbi, Solid State Commun. **74**, 199 (1990).
[26]L. Rimai, M. E. Heyde, and D. Gill, J. Amer. Chem. Soc. **95**, 4493 (1973).
[27]G. P. Brivio and E. Mulazzi, Phys. Rev. B **30**, 876 (1984).
[28]A. C. Albrecht, J. Chem. Phys. **34**, 1476 (1961).
[29]J. Tang and A. C. Albrecht, in *Raman Spectroscopy,* edited by A. Szymanski (Plenum, New York, 1970), p. 33.
[30]H. Kuzmany, P. R. Surján, and M. Kertész, Solid State Commun. **48**, 243 (1983).
[31]T. H. Keil, Phys. Rev. **140**, A601 (1965).
[32]M. F. Granville, B. E. Kohler, and J. B. Snow, J. Chem. Phys. **75**, 3765 (1981).
[33]P. A. Lee, T. M. Rice, and P. W. Anderson, Solid State Commun. **14**, 703 (1974).
[34]E. B. Wilson, J. C. Decius, and P. C. Cross, *Molecular Vibrations* (McGraw-Hill, New York, 1955).
[35]R. E. Peierls, *Quantum Theory of Solids* (Clarendon, Oxford, 1955).
[36]W. P. Su, J. R. Schrieffer, and A. J. Heeger, Phys. Rev. B **22**, 2099 (1980).
[37]H. C. Longuet-Higgins and L. Salem, Proc. R. Soc. London, Ser. A **251**, 172 (1959).
[38]M. Kertész and P. R. Surján, Solid State Commun. **39**, 611 (1981).
[39]P. R. Surján and H. Kuzmany, Phys. Rev. B **33**, 2615 (1986).
[40]J. Kürti and P. R. Surján, in *Electronic Properties of Conjugated Polymers III,* edited by H. Kuzmany, M. Mehring, and S. Roth (Springer-Verlag, Berlin, 1989), p. 69.
[41]J. Kürti and H. Kuzmany, Synth. Met. **43**, 3497 (1991).
[42]R. M. Martin and L. M. Falicov, in *Light Scattering in Solids I,* edited by M. Cardona (Springer-Verlag, Berlin, 1983), p. 79.
[43]R. Loudon, *The Quantum Theory of Light* (Clarendon, Oxford, 1983), p. 312.
[44]H. Kuzmany, *Festkörperspektroskopie, Eine Einführung* (Springer-Verlag, Berlin, 1990), p. 305.
[45]J. Behringer, Z. Elektrochem. **62**, 906 (1958).
[46]C. A. Coulson, Proc. R. Soc. London, Ser. A **207**, 91 (1951).
[47]J. Kürti and H. Kuzmany, Phys. Rev. B **38**, 5634 (1988).
[48]T. C. Clarke, R. D. Kendrick, and C. S. Yannoni, J. Phys. (Paris) Colloq. **44**, C3-369 (1983).
[49]C. R. Fincher, Jr., D. L. Peebles, A. J. Heeger, M. A. Druy, Y. Matsumara, A. G. MacDiarmid, H. Shirakawa, and S. Ikeda, Solid State Commun. **27**, 489 (1978).
[50]J. Kürti and P. R. Surján, J. Chem. Phys. **92**, 3247 (1990).
[51]*Vibrational Intensities in Infrared and Raman Spectroscopy,* edited by W. B. Person and G. Zerbi (Elsevier, New York, 1982).
[52]A. Warshel and P. Dauber, J. Chem. Phys. **66**, 5477 (1977).
[53]H. Kuzmany and P. Knoll, in *Electronic Properties of Polymers and Related Compounds,* edited by H. Kuzmany, M. Mehring, and S. Roth (Springer-Verlag, Berlin, 1985), p. 114.
[54]P. G. Szalay, A. Karpfen, and H. Lischka, J. Chem. Phys. **87**, 3530 (1987).
[55]J. Kürti, H. Kuzmany, and G. Nagele, J. Mol. Electron. **3**, 135 (1987).
[56]P. Vogl and D. K. Campbell, Phys. Rev. Lett. **62**, 2012 (1989).
[57]J. T. Lopez Navarrete, and G. Zerbi, Solid State Commun. **64**, 1183 (1987).